



## Article

**Cite this article:** Hall B, Johnson S, Thomas M, Rampai T (2023). Review of the design considerations for the laboratory growth of sea ice. *Journal of Glaciology* 69(276), 953–965. <https://doi.org/10.1017/jog.2022.115>

Received: 17 November 2021  
Revised: 18 September 2022  
Accepted: 21 October 2022  
First published online: 16 January 2023

### Key words:

Sea ice; sea-ice growth and decay; sea-ice/ocean interactions; solid salts; volume scaling methods

### Author for correspondence:

Tokoloho Rampai,  
E-mail: [tokoloho.rampai@uct.ac.za](mailto:tokoloho.rampai@uct.ac.za)

# Review of the design considerations for the laboratory growth of sea ice

Benjamin Hall<sup>1</sup>, Siobhan Johnson<sup>1,2</sup>, Max Thomas<sup>3</sup>  and Tokoloho Rampai<sup>1,2</sup>

<sup>1</sup>Department of Chemical Engineering, University of Cape Town, Rondebosch, Cape Town 7712, South Africa;

<sup>2</sup>Marine and Antarctic Research Centre for Innovation and Sustainability (MARIS), University of Cape Town, Rondebosch, Cape Town 7712, South Africa and <sup>3</sup>Department of Physics, University of Otago, P.O. Box 56, Dunedin 9054, New Zealand

## Abstract

Sample collection and field studies of sea ice take place under harsh conditions which, combined with the logistical difficulties and high cost of voyages to the polar regions, limits the abilities of researchers to determine its properties. Observations of laboratory-grown sea ice can help quantify important sea-ice properties and incorporate them into numerical models. The growth of laboratory sea ice requires experimental set-ups that consider the complexity of sea-ice growth. Regulation and monitoring of environmental variables allow for growth and melt conditions to be controlled, manipulated and reproduced. Facilities thus vary widely because of differing research objectives. This paper presents a summary of some of the published sea-ice laboratories that study the physical properties of sea ice and an overview of their major design considerations, such as tank size, freezing method and instrumentation. It also discusses how these design considerations were implemented in the set-up of the new sea-ice growth laboratory at the Marine and Antarctic Research for Innovation and Sustainability. This paper should guide others in designing their facilities as well as in their understanding of other facilities for results comparison.

## 1. Introduction

Sea ice is a complex, multi-component, multiphase material consisting of solid ice containing inclusions of liquid brine as well as solid salts and gas bubbles (Hunke and others, 2011). The complexity of sea ice emerges from the proportionality and geometric arrangement of these components which differ according to growth conditions (Weeks, 2010). Under turbulent conditions, sea ice develops from frazil ice crystals which consolidate, and form rounded pieces of sea ice called ‘pancakes’, which in turn consolidate into large sheets (Lange and others, 1989). Calmer conditions lead to the formation of a thin, flexible and continuous ice sheet known as ‘nilas’, which thickens through bottom freezing (Petrich and Eicken, 2010). Sea-ice research has been steadily increasing since the second half of the 20th century and the motivation for such research has been diverse, ranging from offshore oil and gas exploration in the Arctic, to concerns regarding climate change (IPCC, 2007). While these research activities have different focuses, there is often an overlap of the desired properties and research questions.

Sea ice experiences significant property changes once removed from its environment, making it difficult to accurately observe certain properties (Cox and Weeks, 1986). As mentioned by Weeks and Cox (1974), dangerous conditions and harsh environments, combined with the logistical difficulties and high cost of voyages to polar regions limits the abilities of researchers to study these in situ processes, or even to obtain samples for analysis. Laboratory-grown sea ice provides a means of observing these properties of sea ice by enabling its controlled growth under adjustable environmental conditions with tight variable control (Haas, 1999). Laboratory-grown sea ice is saline ice that is grown under a specific set of boundary conditions which mimics that of naturally grown sea ice. It can be used to evaluate and improve computational models for processes such as brine transport (Griewank and Notz, 2013; Turner and others, 2013; Rees Jones and Worster, 2014) and wave–ice interaction (Sutherland and others, 2019). The control of these variables in a stable laboratory environment allows for experimental repeatability, as well as examination of the effect of single variable variation. Study of in situ phenomena such as brine drainage is possible to a greater extent in a controlled environment than in the field (Eide and Martin, 1975). There are some limitations to laboratory-grown sea ice: it generally cannot reach thicknesses typically observed in nature, and tanks are often too small to study important processes (such as pancake ice formation). There have been several studies of sea-ice properties carried out using laboratory-grown sea ice, such as the INTERICE project (Haas, 1999) and the Reduced Ice Cover in the Arctic Ocean (RECARO) project (Wilkinson and others, 2009).

The researchers at the University of Cape Town’s Chemical Engineering Department through the Marine and Antarctic Research Centre for Innovation and Sustainability (MARIS), undertook an investigation of the physical and structural properties of sea ice. In order for this research to be carried out, an appropriate polar laboratory needed to be developed. The initial stages of this development included the creation of an appropriate laboratory set-up. Beyond the early review and directions provided by Weeks and Cox (1974) and the

© The Author(s), 2023. Published by Cambridge University Press on behalf of The International Glaciological Society. This is an Open Access article, distributed under the terms of the Creative Commons Attribution licence (<http://creativecommons.org/licenses/by/4.0/>), which permits unrestricted re-use, distribution and reproduction, provided the original article is properly cited.

[cambridge.org/jog](https://cambridge.org/jog)



design considerations briefly outlined by Thomas and others (2021), no cohesive resource that covered all the factors and considerations involved in the creation of laboratory-grown sea ice was found. As a result, the initial set-up was limited by tank design and instrumentation. As there was insufficient existing literature providing a comprehensive resource for the initial design and set-up of such a laboratory, this paper thus aims to summarise existing literature and to provide a directional guide for those who wish to build and improve their own sea-ice growth set-up.

## 2. Growth of laboratory sea ice

Laboratory-grown sea ice is used by researchers to better understand naturally occurring sea ice and is grown to mimic natural sea ice. It is used to study how it would behave under varying environmental conditions. These conditions include, and are not limited to, the ambient temperature, water temperature, salt content and agitation. These variables may differ to suit the research aims.

### 2.1 Freezing methods

Analogous to the natural conditions in which sea-ice growth is mainly driven by heat loss to the atmosphere, laboratory-grown sea ice is formed by a saline water solution in contact with cold ambient air in the controlled environment, or by contact with cold plates. The growth of laboratory sea ice has been carried out in atmospheric temperatures ranging from  $-5$  to  $-30^{\circ}\text{C}$  using a variety of freezing methods. Roscoe and others (2011) grew laboratory sea ice in temperatures as low as  $-40^{\circ}\text{C}$ ; however, this was specifically to examine the growth of frost flowers. The choice of atmospheric temperature affects the growth rate which in turns affects the sea-ice properties such as crystal size and salinity (Weeks and Assur, 1967). A surface temperature of  $-20^{\circ}\text{C}$  is a popular choice since it mimics natural average winter air temperatures measured in the polar regions and allows for reasonably fast ice growth (Cox and Weeks, 1975; Middleton and others, 2016).

It is common to make use of a temperature-controlled room, that houses a tank filled with a saline solution, where the temperature can be adjusted to the desired atmospheric temperature (Weeks, 1962; Cottier and others, 1999; Loose and others, 2009; Roscoe and others, 2011), with heat transfer taking place between

the cold ambient air and the saline water solution surface. Several of these laboratories are re-purposed refrigeration shipping containers (Light and others, 2015; Marks and others, 2017).

Many experimental set-ups include a fan which blows the cold air above the saline solution surface which enhances circulation, thereby improving the heat transfer rate and homogeneous distribution of cold air (Perovich and Grenfell, 1981; Marks and others, 2017). Insulation of the sides of the tank set-ups is used to limit the heat exchange to the water's surface. Many of these laboratories use floor-based air circulation (Roscoe and others, 2011; Marks and others, 2017), thus further requiring the use of thick insulation at the bottom of the tank. Some refrigeration laboratories require a warming period every few hours to remove ice build-up around the compressor unit (Wiese and others, 2015; Marks and others, 2017). Marks and others (2017) note an increase in the room temperature of up to  $6^{\circ}\text{C}$  during these defrosting periods. Haas (1999) describes the use of the purpose-built, temperature-controlled sea-ice tank facility at the Hamburg Ship Model Basin that consists of a tank with top-down cooling that accomplishes directed cooling at a variety of flow rates. In addition, the use of additional compressors or fans allows their use on a rotational basis; when one undergoes a warming period another keeps the container's temperature at the set temperature, hence removing these defrosting periods. Defrost cycles can be modified in some systems to occur more often and for a shorter period which may reduce the effect on the air temperature inside the laboratory.

For certain studies, such as mechanical testing or investigation of growth rates, it is optimal to procure samples that are grown at a single, stable temperature such that the effect of temperature can be selectively examined (Schwarz and others, 1981). This can be accomplished using a cold plate in direct contact with the saline solution. Cold plates consist of a machined metal plate that is placed over the saline solution and in direct contact with it (Fig. 1). The plate has channels through which a coolant is pumped, allowing very stable control of temperature, with fluctuations as low as  $0.1^{\circ}\text{C}$  (Golding and others, 2014).

The cold plate may replace the need for convective atmospheric cooling but housing the experimental system in a temperature-controlled room is still preferable (Notz and Worster, 2006). Cold plates are the most precise cooling method if temperature control is a key concern. The cold plate, however, does not allow a natural sea-ice freeboard and requires a pressure



Fig. 1. Cold plate used for controlled cooling in direct contact with the solution sea ice (Schulson and others, 2015).

relief system to account for the density change during sea-ice growth (Notz and Worster, 2006). Furthermore, it adds complexity to the measurement systems as the instrumentation has to pass through either the cold plate or tank sides to measure tank conditions, rather than the exposed water surface.

In some studies, experimental set-ups deviating from natural growth conditions were necessary for the research objectives such as testing of the salinity measurement harp (Shirtcliffe and others, 1991; Notz and Worster, 2006). Details of these set-ups exceed the scope and are not further discussed in this review.

In addition to cooling from the top surface, control of the temperature or heating rate is typically required for the underlying saline solution (Weeks and Cox, 1974; Roscoe and others, 2011; Wiese and others, 2015; Marks and others, 2017). A heat input prevents undesired supercooling from occurring, and further ensures top-down cooling from the surface of the saline solution. Wiese and others (2015) found that a heat input of  $15 \text{ W m}^{-2}$  via the installation of a heating wire at the bottom of the tank was sufficient to prevent supercooling.

## 2.2 Tank configuration and material

Laboratory-grown sea ice has been grown in tank vessels ranging from less than a litre (Eide and Martin, 1975), to tanks >1 million litres (Haas, 1999). The first design consideration is whether the tank will be cooled using ambient temperatures, or a cooling mechanism. Some facilities, such as the 589 000 L tank at the Sea-ice Environmental Research Facility (SERF), University of Manitoba, or the Geophysical Institute, University of Alaska Fairbanks are in areas where ambient temperatures are below freezing for sustained portion of the year (Hare and others, 2013; Galley and others, 2015; Oggier and others, 2019). This allows them to have outdoor tanks which are cooled using ambient temperatures which saves on the cooling costs of electrical cooling methods. However, it is sometimes preferable to have the ability to supplement this natural ambient cooling using additional chillers, such as the Ohmsett tank, at the National Oil Spill Response Research and Renewable Energy Test Facility, which can keep the saline solution at freezing point (Buist and others, 2011).

The choice of tank size, configuration and freezing method is largely influenced by research aims and budget. The properties of sea ice are not independent of tank size and there are advantages and disadvantages to whichever size is chosen. Smaller tanks are cheaper and are useful for analysis of structure and chemical composition, where the formation of large samples is not crucial (Weeks and Cox, 1974). Larger tank sizes, together with the shape of the vessel, are useful for the implementation of wave pumping and circulation, however large wave pumping forces are needed to evenly distribute circulation and wave motion. The shape of the tank is important to consider if wave pumping or agitation is being incorporated as undesired water circulation patterns may arise (Timmons and others, 1998). Additionally, large tanks generate a greater number of samples which is recommended for testing of properties that require a minimum sample size and fixed dimensions, such as testing of mechanical properties (Schwarz and others, 1981).

Rounded tanks have been found to minimise the stress on the tank walls (Perovich and Grenfell, 1981). A variety of materials have been used for tank construction. Marks and others (2017) and Golding and others (2014) chose to construct their tanks from plastic, since this is a cost-effective, lightweight and non-reactive material.

Weeks (1962) used a steel tank coated in an anticorrosion paint due to the salt in the saline solution. The metal would also have conducted temperatures extremely well, which may exacerbate any effects at the tank sides. Indeed, it was mentioned

by the authors in a later paper (Cox and Weeks, 1975) that the sea ice was thicker at the tank sides, suggesting a greater degree of cooling near the walls. Shaw and others (2011) used a square stainless-steel tank to examine the diffusive transport of atmospheric halocarbons through sea ice; in this case, stainless steel was used since it would not interact with the halocarbons.

Glass tanks are suitable for experiments that prioritise visualisation of the laboratory-grown sea ice (Eide and Martin, 1975; Middleton and others, 2016). Concrete is also commonly used for large tanks with length on the order of 10 m (Rysgaard and others, 2014).

Insulating round tanks provides some challenges because the insulation must be flexible to tightly fit around the curved sides. Both Weeks (1962) and Marks and others (2017) used neoprene sheets adhered to the tank wall to provide a first insulation layer. However, their next layers differ, as Weeks (1962) used glass wool and tar paper, while Marks and others (2017) built up a square wooden box fitted with polystyrene sheets. A simple and novel solution to both tank and insulation was used by Light and others (2015), who grew sea ice in a commercially available, insulated square tank primarily used for food transport. Square tanks have also been commonly used, either made of glass (Thomas and others, 2021), plexiglass (Eide and Martin, 1975; Middleton and others, 2016), steel (Shaw and others, 2011) and concrete (Rysgaard and others, 2014).

## 2.3 Agitation

Haas (1999) points out that growth rates and temperature gradients for laboratory-grown sea-ice set-ups are much greater than those found in naturally occurring sea ice. Therefore, some laboratory-grown sea-ice set-ups use a system to circulate or agitate the underlying saline solution to ensure that temperature and solution salinity stratification does not occur while the sea ice grows. This mixing can be provided by using a pumped water circulation system (Marks and others, 2017) or aquarium impeller pumps (Roscoe and others, 2011; Wiese and others, 2015; Thomas and others, 2021). The geometry of tanks influences mixing, and different geometries will require different mixing set-ups and pump placements to ensure optimal mixing. Circular mixing works best in round tanks with a single pump able to provide good mixing when placed tangentially to the tank wall to create a circularly orientated flow (Timmons and others, 1998). The primary tangential flow pattern generates a secondary, radial flow that creates bottom circulation towards the tank centre. However, Timmons and others (1998) did note that there could be a dead zone formed near the centre of the tank where low fluid velocities result in poor mixing (Fig. 2).

Square tanks do not work well with circular flow and have dead zones in their corners (Lekang, 2013). A general configuration for the pump placement in a square tank is to use two pumps, and to place them diagonally across from each other in the tank corners (Loose and others, 2011; Shaw and others, 2011).

The agitation rate is important as Langhorne and Robinson (1986) found that a significant degree of horizontal alignment within the crystal *c*-axes could be seen under growth conditions with currents faster than  $10 \text{ mm s}^{-1}$ . This crystal alignment was due to a current formed within the tank from the agitation (Stander and Michael, 1989; Cottier and others, 1999). Currents also affect the sea-ice porosity, with stronger currents resulting in smaller pores but greater pore densities (Eicken and others, 2000).

## 2.4 Pressure relief and formation of free-floating ice

Sea ice has a density less than that of sea water, instigating a volume increase upon freezing. Natural sea ice floats, maintaining a

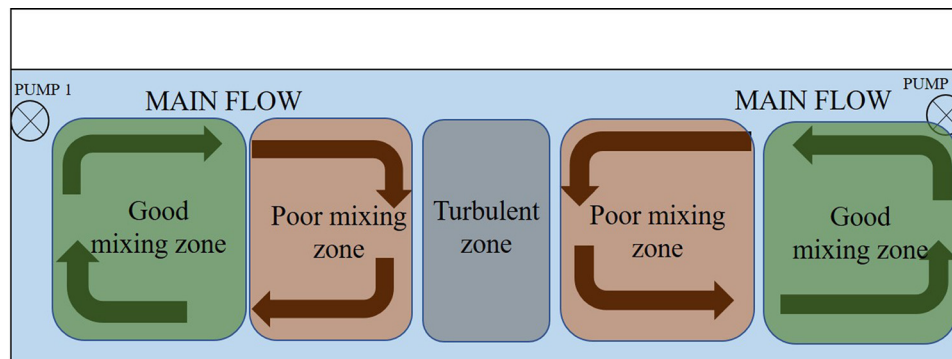


Fig. 2. Schematic diagram of flow pattern generated with primary tangential mixing in a round tank. Adapted from Timmons and others (1998).

certain freeboard. Within a closed volume system, this volume increase can lead to rupture of a tank, damage to instrumentation or falsification of measurements through flooding of the ice surface. Maintaining the freeboard within the tank is important to avoid this. This can be achieved by a pressure-relief pipe or the creation of free-floating sea ice. Side heating of the tank walls may prevent sea ice from freezing to the walls and form free-floating sea ice (Thomas and others, 2020). Side heating should be considered carefully as extensive heat input can prevent or reduce sea-ice growth. Smooth glass tanks prevent sea ice forming against the tank walls with a lower side heating input (Wiese and others, 2015; Thomas and others, 2021). Any irregularities of the tank material will also affect natural floating of the sea ice. The choice of free-floating sea ice affects the mounting of the instrumentation, since free floating sea ice will result in the surface level of the ice moving upwards due to volume increase.

Systems with capped, top-down cold plates cannot maintain free-floating sea ice and have often used pressure relief pipes (Cox and Weeks, 1975; Golding and others, 2014). No valve is required in such set-ups, since if the height of the relief pipe is above the water surface, no drainage will occur. The water head will naturally increase above the sea-ice level to equalise pressure as the sea ice grows downwards. The same system of pressure relief has been used in open tanks where the sea ice is constrained against the tank walls (Weeks, 1962) and the overflowing water in the pressure relief pipe was routed into a secondary tank or basin. It is crucial that such pipes are insulated to prevent freezing and subsequent blockage of the pressure relief pipe (Weeks, 1962; Schulson and others, 2015).

Weeks (1962) found that using insulation only was insufficient to prevent freezing of the pressure relief pipe, and thus used a heated wire wrapped around the pipe. Style and Worster (2009) prevented pressure build-up in their tank by drawing liquid out of a submerged methanol bladder, which allowed them to prevent flooding of the sea-ice surface. Roscoe and others (2011) used plastic envelopes filled with bubble wrap that were clamped to the tank walls slightly below the sea ice which minimised the pressure build-up. Shaw and others (2011) also used a similar air-compressible system for pressure relief.

### 2.5 Solution preparation and salinity

The formation of laboratory-grown sea ice requires a solution of salt and water, ideally one that mimics natural sea water found in the polar regions. Nomura and others (2006) and Weissenberger and others (1992) both made use of available natural sea water for their growth set-ups. However, as noted by Weeks and Cox (1974), this can be expensive if one is located far from the coast and natural sea water may not have the required salinity for the planned experiments. Additionally, when growing sea ice in

small tanks, the water should have a lower starting salinity to obtain the a bulk salinity of the resulting sea ice that resembles that of natural sea ice (Schulson and others, 2015). This is due to the brine drainage from the newly grown sea ice which increases the salinity of the underlying saline solution, which in turn forms more saline sea ice.

To overcome the difficulties of using natural sea water, one can make the saline solution using deionised water or tap water and salts. Some experimental set-ups have used sodium chloride for the formulation of their saline solution (Weeks, 1962) while others have used water with a representative sea-water composition (Cottier and others, 1999; Papadimitriou and others, 2004; Hare and others, 2013; Marks and others, 2017).

Typical values for the starting solution salinities range from 17.5 (Schulson and others, 2015) to 32 g kg<sup>-1</sup> (Marks and others, 2017). The resultant sea-ice bulk salinities within these studies show a much smaller range. The aforementioned solution salinities resulted in sea-ice bulk salinities of 5 and 7 g kg<sup>-1</sup> respectively. Schulson and others (2015) recommend that the required solution salinity should be experimentally determined for different set-ups. Murdza and others (2021) grew laboratory sea ice at a starting solution salinity of 17.5 and 35 g kg<sup>-1</sup> at a temperature of -20°C. It was reported that the final sea-ice bulk salinities were 3 and 6 g kg<sup>-1</sup> respectively, which both fall within the range of natural sea-ice bulk salinity (Weeks and Ackley, 1986; Weeks, 2010). However, under mechanical flexural test conditions, sea-ice samples grown with different initial salinities performed differently under cyclical loading with different flexural strengths (Murdza and others, 2021).

### 2.6 Seeding for selective sea-ice growth

The freezing point of a saline solution refers to the thermodynamically defined temperature at which sea ice will begin to form from a saline solution. The saline solution, however, may be supercooled and remain in its liquid phase at a temperature lower than what the thermodynamic limit predicts (Freitag, 1999). In such cases, a process of nucleation needs to occur for ice to form.

Nucleation can take place as either primary or secondary nucleation. Primary nucleation refers to the spontaneous nucleation of sea ice from solution and takes place at temperatures lower than the thermodynamically predicted crystallisation temperature. Secondary nucleation involves the addition of a small number of sea-ice crystals into the solution, providing a site for sea-ice nucleation. Secondary nucleation is possible within a very small degree of supercooling. This process of adding small amounts of sea-ice crystals, or parent material is known as seeding (Randall and others, 2009). The formation of natural sea ice commonly occurs through a natural process of secondary

nucleation from readily available heterogeneous nuclei such as dust or aerosol particles (Weeks, 2010) as well as from snowfall (Murdza and others, 2021) which promotes granular sea-ice formation at the surface before columnar textures form under calm conditions. Tucker and others (1987) reported that an absence of this natural seeding has been found to occasionally occur on lakes, in Arctic melt ponds and in polynya. Increased agitation of the water body also increases the probability of natural seeding (van der Elsken and others, 1991; Liang and others, 2004; Ye and Doering, 2004). Therefore, in laboratory-grown sea ice, where natural secondary seeding is not present, it is common to manually seed the saline solution with ice shavings or milled sea-ice specimens at the predicted freezing point to promote sea-ice growth and control grain size (Cottier and others, 1999; Kim and others, 2006; Golding and others, 2014).

Seeding has been accomplished using two methods. Cottier and others (1999) and Dempsey and others (1989) used spray seeding, where a spray bottle of supercooled deionised water was sprayed over the water surface. The water droplets crystallised upon contact with the cold ambient air and provided crystals for nucleation to occur. Another method is to sprinkle crushed sea ice over the saline solution surface while it is at its freezing point temperature (Barrette and Jordaan, 2001; Golding and others, 2014).

### 3. In situ measurement systems

#### 3.1 Temperature measurement

Sea-ice temperature is one of the most important variables to record during sea-ice growth. Parameters such as growth rate and brine volume depend on the temperature. A record of temperature enables a description of the history of the sea-ice growth, which allows for a better understanding of its properties. Haas (1999) remarked that the ability to record this temperature history easily is one of the greatest advantages of laboratory-grown sea ice. Temperature of both, the underlying saline solution and the sea-ice temperature, can be measured using one of the three popular sensor types, depending on the property of interest and the degree of accuracy required. These are thermocouples, thermistors and resistive temperature detectors (RTDs).

The most common sensor type used for temperature measurement in laboratory sea-ice set-ups is a thermistor (Eide and Martin, 1975; Perovich and Grenfell, 1981; Cottier and others, 1999; Haas, 1999; Wiese, 2012). Thermistors are comparatively low in cost, with a high accuracy and small footprint. Thermistors have been used by Lake and Lewis (1970) to track brine movement by analysing temperature fluctuations within sea ice, taking advantage of the small size of the probe instruments. Unfortunately, thermistors experience drift over time, in the region of  $0.2^{\circ}\text{C a}^{-1}$ . They therefore require frequent calibration to ensure their measurement accuracy (Wiese, 2012). The two most common types of RTD sensors are PT100 or PT1000, commonly used for water and air measurement and can be used in hand-held measurement devices. RTDs have long response times, taking between 1 and 50 s to respond to temperature changes. However, they can be accurate, with class A PT100s rated to an accuracy of  $0.15^{\circ}\text{C}$ . In addition, their measurement is highly stable over time, with a drift of  $0.05^{\circ}\text{C a}^{-1}$ . Thermocouples are simple and have a robust design that allows for measurement across a large range of temperatures (Omega, 2019). However, associated accuracy is  $0.5^{\circ}\text{C}$  at best and can cover a wide range of temperatures (Omega, 2019). Galley and others (2015), Marks and others (2017), Nomura and others (2006), Shokr and others (2009) and Weeks (1962) all made use of the thermocouples' simple design in their experiments.

Spatial resolution is an important consideration for placement of temperature probes for vertical temperature profiles. The vertical span of the sensors should cover the full thickness of the sea ice that is to be grown, such as in a vertical chain of probes. Reported vertical resolutions range from 0.5 to 8 cm (Notz and Worster, 2008; Wiese, 2012; Galley and others, 2015; Wiese and others, 2015; Thomas and others, 2021). Horizontal spacing of sensors (for multiple vertical profiles) can be used to investigate heterogeneities in the sea ice. However, the area of sea ice that can be destructively sampled without damaging sensors is reduced when more sensor arrays are deployed, and this may limit the number of vertical profiles in small tanks.

#### 3.2 Salinity measurement

Liquid salinity is commonly calculated from measurements of conductivity and temperature, which are converted to salinity using the thermodynamic equation of seawater (TEOS-10). Salinity measurement can differ when observing the salinity of the solution or water and when observing the salinity within the sea ice. A common method in sea-ice labs is the use of a CTD in the surrounding saline solution, an oceanographic instrument array that measures conductivity, temperature and depth (Wiese, 2012). These are precise, commercially available instruments, providing an accurate measurement of the solution salinity. Another method to measure solution salinity is the use of small sampling tubes placed at the desired measurement location (Notz and Worster, 2008; Garnett and others, 2019). These tubes can be run to outside of the tank, where a syringe can be used to draw a sample that can then be measured using a salinometer to determine its salinity. While simple and low cost, this method has a low temporal resolution and requires the sample lines to be kept heated to prevent unwanted ice build-up and requires the extracted volume to ideally be added back into the system so as not to have any effect on freeboard (Thomas and others, 2020). Weeks and Cox (1974) suggested that if the solution is well mixed during sea-ice growth, and at constant pressure, the solution can be assumed to be at freezing point and thus salinity can be calculated using the salinity–temperature relationship. While very simple, it does involve a few assumptions such as the absence of supercooling or sea-ice formation at the temperature measurement point and can only be used once sea-ice formation has begun.

For sea-ice bulk salinity, Cox and Weeks (1975) presented a method that used a radioactive tracer that was added to the initial saline solution. By using a scintillation detector, the location and relative salinity within the sea ice could be determined. However, a disadvantage of this method is the additional safety concerns and precautionary measures instigated by the radioactive element. A salinity harp developed by Notz and others (2005) can also be used for continuous sea-ice bulk salinity measurement (Notz and Worster, 2006). The salinity harp consists of a vertical array of wire pairs that are spaced at roughly centimetre vertical resolution. The resistance between each wire pair can be measured allowing derivation of the sea-ice liquid fraction and a co-located temperature measurement allows the brine salinity to be calculated. The salinity harp therefore provides profiles of the liquid fraction, brine salinity and bulk salinity of the sea ice. Uncertainties on the salinity harp measurement are further discussed in Zeigermann (2018) and Fuchs (2017).

In the absence of a non-destructive method, the bulk sea-ice salinity can be measured by removing a sea-ice sample, cutting it into vertical sections and melting each section down before using a salinometer to measure the salinity of the meltwater (Weeks, 2010). This is the most common method to measure sea-ice bulk salinity, both in field and laboratory-derived samples.

In addition to the loss of the temporal evolution of the sea-ice bulk salinity profile, this method's primary drawback is the loss of brine during extraction, which affects the accuracy of the result (Thomas and others, 2021).

### 3.3 Sea-ice thickness

Measurement of the sea-ice thickness is important to determine its growth rate. The simplest method of measuring sea-ice thickness is by visual inspection, which can be used if the tank is made of transparent material such as glass or plexiglass (Wiese and others, 2015; Thomas and others, 2021). A removable square of the insulation can be cut, allowing for a measurement to be taken using a rule stuck to the side of the glass. However, if the tank is opaque or the insulation cannot easily be removed, then other methods are available. Weeks (1962) measured sea-ice thickness using a metal rod with a cross bar that was frozen into the sea ice. The rod was heated to enable it to slide freely within the sea ice, and by pulling the cross bar up to the underside of the sea-ice surface, a measurement of sea-ice thickness could be obtained. The salinity harp designed by Notz and others (2005) also allows for the measurement of sea-ice thickness and records the data continuously. The linear temperature profile within sea ice provides a reasonable approximation up to thicknesses of 0.8 m (Feltham and others, 2006). This linear trend is seen in laboratory-grown sea ice as well by Marks and others (2017) as a means of continuous sea-ice thickness approximation.

### 3.4 Sea-ice characterisation

With the growth of laboratory sea ice, analysis of the specimens is needed to understand and validate whether the growth parameters are producing sea ice that is similar to natural sea ice. Temperature, salinity and crystal structure are commonly measured properties of sea ice that can assist in characterisation.

Vertical temperature profiles of growing sea ice have an approximately linear relationship with depth, with the lowest temperature at the surface of the sea ice and the highest temperature at the ice–ocean interface (Weeks and Ackley, 1986; Weeks, 2010). This recognisable profile is a simple way to initially determine whether the laboratory sea ice was grown under top-down cooling conditions.

The vertical salinity profile of sea ice can differ depending on its growth stage (Eicken, 1992). Typically, however, C-shaped and S-shaped profiles are found in growing winter sea ice. These profiles have a high salinity measurement at the sea-ice–ocean interface and a low bulk salinity throughout the middle of the sea ice. The C-shaped profile has a high salinity at the sea-ice surface while an S-shaped profile has a slight decrease in salinity at the surface followed by a high salinity measurement, just below the sea-ice surface (Eicken, 1992). Similarly, to the temperature profile, these salinity profiles are distinct and can validate the growth conditions as brine convection was present within the sea ice to form such profiles.

Analysis of crystal and grain structure in sea ice is commonly carried out using cross-polarisation imaging techniques, which views a thin section of a sample between two cross-polarised lenses (Weeks and Ackley, 1986; Weeks, 2010). Preparation of a thin section has typically been carried out using a microtome and viewed with a Rigsby stage to determine the *c*-axis orientations and crystal grain sizes (Langway, 1958; Hill and Lasca, 1971) in order to characterise the sea ice in terms of its structure, which is closely linked to its growth conditions. Crystal sea-ice textures such as granular and columnar are the two dominant and recognisable textures in natural sea ice and are indicative of turbulent and calm growth conditions respectively (Weeks and

Ackley, 1986; Weeks, 2010). Furthermore, imaging techniques such as micro-computed tomography ( $\mu$ CT) imaging and magnetic resonance imaging, can be employed to visualise the internal structure of the sea ice: its porosity, brine connectivity and brine channel structure (Galley and others, 2015; Middleton and others, 2016).

## 4. Summary of existing set-ups

The existing laboratory sea-ice growth set-ups vary considerably in research aims and vessel configuration. Table 1 summarises some of the published laboratory sea-ice set-ups and highlights the differences between them. We found these facilities by manually searching existing literature. The list captures the breadth of approaches in the literature but is not exhaustive. The included facilities were limited to those who primarily focused on sea-ice physics or its material properties. Ship design and offshore engineering as sole motivation for laboratory sea-ice research was excluded from this study. The differences between these facilities are important to note within the context of the facility's research and emphasises the need to review and detail the process of designing and setting up a general sea-ice growth system based on the available resources and research outcomes.

## 5. Facility description of MARiS sea-ice laboratory

### 5.1 Tank design

Using the design considerations reviewed, the polar laboratory at the University of Cape Town was set-up for laboratory sea-ice growth to investigate the physical, structural and mechanical properties of sea ice and its relationship with its growth conditions. A refrigerated container was used to house the designed tank and to create cold atmospheric temperatures for the freezing of the saline solution. The designed system consisted of a 400 L circular, high-density polyethylene (HDPE) plastic tank with a height and diameter of 0.8 m (Fig. 3), which was large enough to obtain sufficient samples for analysis and remained affordable. As wave pumping was not considered as part of the experimental plan of this laboratory, a circular tank was chosen. The tank's wall was covered with a thin layer of closed-cell neoprene and a layer of foil to promote even heat distribution from a heating tape which was wrapped around the foil layer and covered with thick plastic wool insulation. The side heating, provided by the  $65 \text{ W m}^{-1}$  waterproof heating tape, was wrapped repeatedly around the tank and provided a small heat input to maintain the boundary conditions.

The instrumentation within the tank can be seen in Figure 4. The cooling unit within the laboratory was to the right of the tank such that the direction of cold air flow and such that the predominant cooling was from this direction. Occasionally, a fan was placed from the opposite direction, providing air flow over the tank surface. The presence of wind flow on the water's surface created mixing of the surface such that nucleation occurred faster. The velocity of the air flow from the fan was a feature of the apparatus available and was not chosen to emulate strong wind conditions. Aquarium pumps were placed in the tank for continuous mixing of the solution throughout the experiment. These pumps were located at a depth of 0.45 and 0.7 m from the water surface, with P1 at a depth of 0.7 m located tangentially to provide tangential mixing as described by Timmons and others (1998). P2 at a depth of 0.45 m was directed radially, on a pulse cycle to create random flow and counteract the formation of dead zones that may occur from tangential flow patterns (Timmons and others, 1998). Pump flow rates were set to  $100 \text{ L h}^{-1}$  for P1 and  $50 \text{ L h}^{-1}$  for P2. The pumps remained on for

**Table 1.** Summary of some of the existing laboratory-grown sea-ice system set-ups and design parameters

Facility name	Association	Location	Research	Indoor/ outdoor	Tank capacity L	Dimensions (L × W × H) m	Tank shape	Material of construction
Cold Regions Research and Engineering Laboratory (CRREL)	US Army Cold Regions Research and Engineering	Hanover, New Hampshire	Mechanical, physical	Indoor	799 000	37 × 9 × 2.4	Rectangular	Concrete
Roland von Glasow Air-Sea-Ice Chamber	University of East Anglia	Norwich, England	Physical, frost flowers, gaseous exchange	Indoor	3700	2.4 × 1.4 × 1.1	Rectangular	Glass
Sea-Ice Environmental Research Facility (SERF)	University of Manitoba	Manitoba, Canada	Physical, brine channel, mechanical	Outdoor	589 000	23.3 × 9.2 × 2.75	Rectangular	Concrete
Arctic Environmental Test Basin (HSVA)	Hamburg Ship Model Basin	Hamburg, Germany	Physical, mechanical, wave dynamics	Indoor	215 000	30 × 6 × 1.2	Rectangular	Concrete
Cold Room Laboratory	University of Cape Town	Cape Town, South Africa	Physical, brine channel, mechanical	Indoor	352	0.8D × 0.7H	Round	Plastic
Sea-ice Laboratory	Royal Holloway University	London, England	Physical	Indoor	1900	1.32D × 1.39H	Round	Plastic
Polar Science Centre	University of Washington	Seattle, Washington	Physical, mechanical	Indoor	1690	1.22 × 1.12 × 1.24	Rectangular	Plastic
Sea-ice-Wind-Wave-Interaction Laboratory (SIWWI)	University of Melbourne	Melbourne, Australia	Physical, wave dynamics	Indoor	4200	14 × 0.75 × 0.4	Rectangular	Concrete
Max Planck Institute for Meteorology	Max Planck Institute for Meteorology	Hamburg, Germany	Physical, brine evolution	Indoor	1540	1.94 × 0.66 × 1.2	Rectangular	Glass
Ice and Environmental Laboratory	Leeds University	Leeds, England	Physical, gaseous exchange, frost flowers	Indoor	240	1.5 × 0.8 × 0.2	Rectangular	Stainless steel
Clarkson University Cold Room	Clarkson University	Potsdam, NY	Physical, permeability	Indoor	384	0.8 × 0.8 × 0.6	Rectangular	Plastic
Geophysical Institute of the University of Alaska Fairbanks	University of Alaska	Fairbanks, Alaska	Physical	Outdoor	360	0.6 × 0.6 × 1	Rectangular	Concrete
University of Alberta Cold Room Facility	University of Alberta	Alberta, Canada	Physical	Indoor	1440	1.2 × 0.8 × 1.5	Rectangular	Glass
Ice Research Laboratory	Dartmouth College	Hanover, New Hampshire	Physical, mechanical	Indoor	946	91.4D × 121.9H	Round	Nalgene
Aalto Ice and Wave Tank	Aalto University	Finland	Physical, wave dynamics	Indoor	4 480 000	40 × 40 × 2.8	Rectangular	Concrete
Cold Laboratory of University Centre in Svalbard	University Centre of Svalbard	Svalbard, Norway	Physical	Indoor	1050	1.5 × 1 × 0.7	Rectangular	Metal
Facility name	Heating	Saline solution	Agitation method	Publications				
Cold Regions Research and Engineering Laboratory (CRREL)	Side heating	Artificial sea	Wave generator	Hirayama (1983), Buist and others (2011), Oggier and others (2019)				
Roland von Glasow Air-Sea-Ice Chamber	Side heating	Artificial sea	Pumps for water mixing	Garnett and others (2019), Thomas and others (2021)				
Sea-ice Environmental Research Facility (SERF)	Bottom heating	Artificial sea	n/a	Hare and others (2013), Rysgaard and others (2014), Galley and others (2015), Crabeck and others (2016)				
Arctic Environmental Test Basin (HSVA)	Side and bottom heating	Artificial sea	n/a	Cottier and others (1999), Haas (1999), Shen and others (2003), Sammonds and others (2017), Li and Lubbad (2018), Cheng and others (2019), Oggier and others (2019), Li and others (2021)				
Cold Room Laboratory	Side and bottom heating	Artificial sea	Pressure pipe relief	This paper				
Sea-ice Laboratory	Bottom heating	Artificial sea	Water mixing	Marks and others (2017)				
Polar Science Centre	Side heating	Artificial sea	n/a	Light and others (2015)				
Sea-ice-Wind-Wave-Interaction Laboratory (SIWWI)	n/a	Artificial sea	Wave generator	Nelli and others (2017), Dolatshah and others (2018), Alberello and others (2019)				
Max Planck Institute for Meteorology	Side and bottom heating	Artificial sea	n/a	Naumann and others (2012), Wiese and others (2015)				
Ice and Environmental Laboratory	bottom heating	Artificial sea	n/a	Roscoe and others (2011)				

(Continued)

Table 1. (Continued.)

Facility name	Heating	Volume expansion method	Saline solution	Agitation method	Publications
Clarkson University Cold Room	Side and bottom heating	Methanol-filled bladder	Artificial sea	Fan	Kawamura and others (2006)
Geophysical Institute, University of Alaska Fairbanks	Side and bottom heating	n/a	Artificial sea	Water mixing	Backstrom (2007), Gully and others (2007), Bullock and others (2017), Oggier and others (2019), Dilliplaine and others (2021)
University of Alberta Cold Room Facility	Side heating	n/a	Artificial sea	Water mixing	Ghobrial and others (2012), McFarlane and others (2015), Schneck and others (2019)
Ice Research Laboratory	n/a	n/a	Artificial sea	n/a	Kuehn and others (1990), Kuehn and Schulson (1994)
Aalto Ice and Wave Tank	n/a	n/a	Artificial sea	Wave generation	Passerotti and others (2020), Passerotti and others (2022)
Cold Laboratory of University Centre in Svalbard	Side and bottom heating	Air balloon	Artificial sea and sea water	Water mixing	Marchenko and others (2011), Bogorodskiy and Marchenko (2014), Marchenko and others (2016), Rabault and others (2019), Marchenko and others (2021)

the duration of sea-ice growth and their heat input was assumed to be negligible. Ambient temperature was measured with a PT100 probe placed 0.01 m above the solution surface. The sea-ice temperature was measured with two temperature chains at position  $T_{i,1,2}$ . Two vertical chains for temperature measurement were used to monitor horizontal heterogeneities in temperature to ensure that cooling was occurring at the same rate on the horizontal plane. These chains consisted of eight temperature probes, at depths of 0.01, 0.03, 0.05, 0.08, 0.13, 0.18, 0.25 and 0.3 m. Further probes were located at 0.45 and 0.70 m, to measure the underlying solution temperature. All temperature probes were class A Pt100 ( $\pm 0.15^\circ\text{C}$ ) and were connected to a Campbell Scientific CR5000 datalogger. Temperature was recorded every 5 min. Typical sea-ice growth for sufficient thickness for sampling took  $\sim 10$  d, thus 5 min intervals was deemed a sufficient interval to capture the temperature changes and profiles in the tank. A flexible, PVC pipe with wire reinforcing was used for pressure relief to prevent tank rupture and equipment damage from excessive pressure build-up. It exited from the bottom of the tank into a smaller, overflow vessel and was located at the position indicated by  $S_p$ , at 0.7 m below the solution surface. Heating tape was also incorporated at the bottom of the tank to prevent convective cooling from the beneath the tank. The bottom and side heating coils were set to the freezing point of the saline solution. A similar heating coil and relay was used within the pressure relief pipe to prevent freezing and blocking of the pipe during experiments.

Once set-up was complete, the laboratory temperature was set to the desired temperature and the experiment ran until the sea ice reached a desired thickness. Defrost cycles were part of the refrigerated container's operation and occurred once every 24 h. This defrosting of the compressor unit brought the ambient temperature of the laboratory up to  $\sim -5^\circ\text{C}$ .

### 5.2 Sea ice sampling and techniques

Sampling was carried out using a modification of the protocol described by Cottier and others (1999). Blocks of sea ice were cut using an auger and saber saw to outline the sample sizes. The blocks were then removed by inserting a wire underneath the sea ice to lift the sample clear. While Cottier and others (1999) provided a method for entrapping the brine and preventing brine drainage with sampling, the protocol would call for a large area of the tank to be taken up, thus limiting the number of samples available for study, and therefore was not applied.

### 5.3 Sea ice physical properties

The following results are those of an experimental run that grew laboratory sea ice at  $-20^\circ\text{C}$  ambient temperature with a starting solution salinity of  $28\text{ g kg}^{-1}$ . The sea ice grew to a thickness of 23 cm over a period of 160 h. It was experimentally determined that a starting solution salinity of  $28\text{ g kg}^{-1}$  resulted in a sea-ice bulk salinity between 7 and  $15\text{ g kg}^{-1}$  for this tank set-up. These preliminary results aim only to showcase that the tank set-up, as described, can successfully grow sea ice that mimics natural sea ice, particularly in its general temperature profile, salinity profile and internal structure.

The sea-ice temperature profiles followed a linear trend (Fig. 5a) with depth as described in both laboratory-grown sea-ice experiments by Marks and others (2017), Weeks (1962) and Wiese (2012) as well as those found in natural sea ice (Weeks and Ackley, 1986; Timco and Weeks, 2010). This suggests an accurate representation of the unidirectional bottom-up heat flux as experienced under natural conditions (Maykut and Untersteiner, 1971). Figure 5a shows the initial uniform cooling of the saline solution before the freezing point was reached.



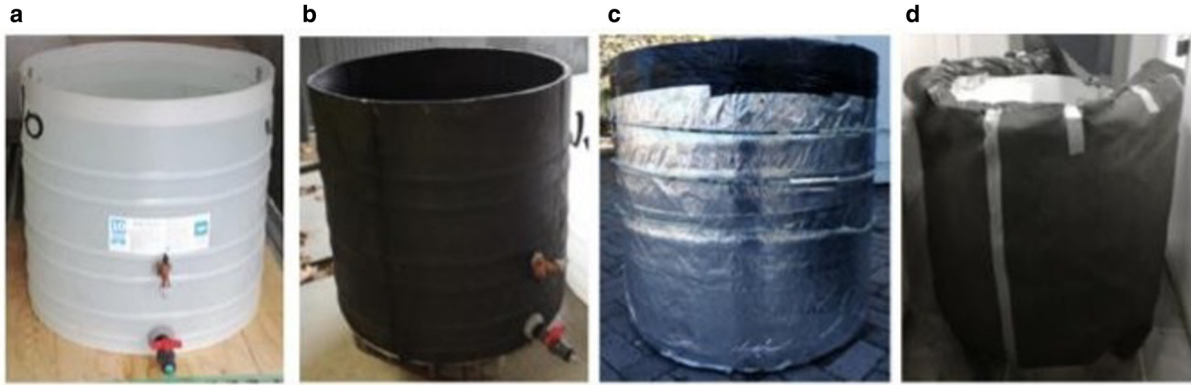


**Fig. 3.** Tank layers: (a) cut HDPE tank, (b) insulated with 3 mm rubber foam, (c) covered with foil for heat conduction from side heating and (d) final tank with outer 135 mm plastic wool insulation.

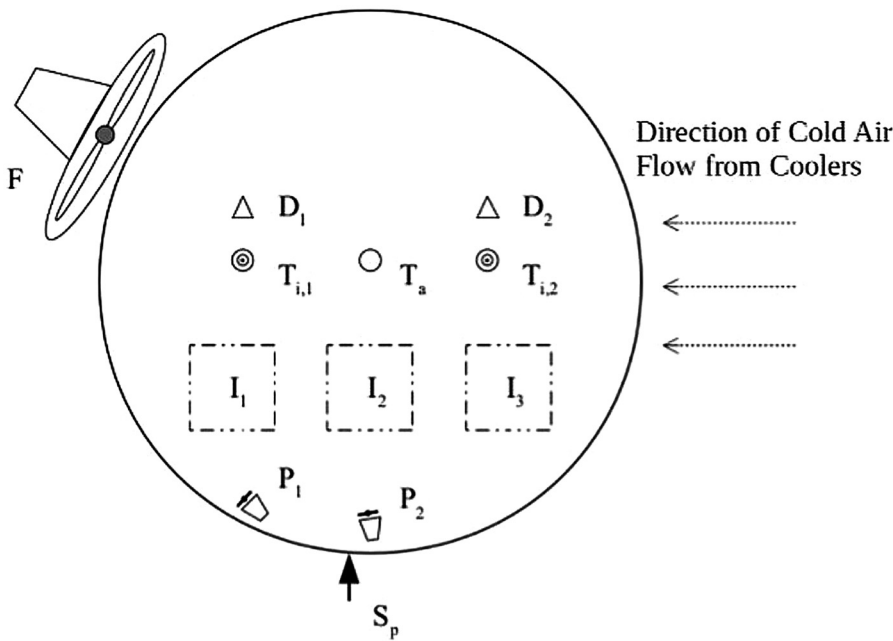


**Fig. 4.** Schematic diagram of experimental set-up, showing locations of fan (F), pressure relief pipe (Sp), pumps (P1-2), manual ice depth measures (D1-2), in-ice temperature chains (Ti;1-2), ambient temperature (Ta) and ice samples (I1-3).

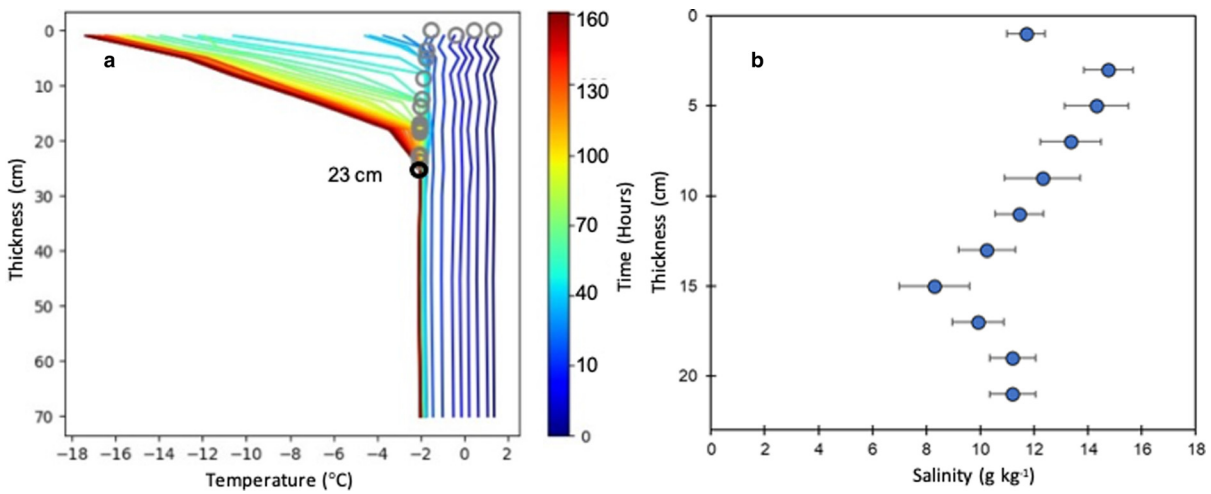


**Fig. 5.** (a) Thickness versus temperature profile of laboratory sea ice during experiment, showing linear sea-ice temperature profile, with the approximate sea ice-solution interface point shown with open circles. The final open circle at the end of the 160 h reports a thickness of 23 cm. (b) Bulk salinity profile of laboratory sea ice with thickness at the end of the experiment.

After sea-ice growth began, the temperature profile for the underlying solution remained vertical and showed only a small decrease in temperature for the remainder of the growth experiment. The

temperature profile within the laboratory sea ice can be clearly seen by the portion of the profile in Figure 5a with a lower gradient, starting from the coldest temperature at the sea-ice surface to

the warmer underlying ice–solution interface. As the experiment progressed, the portion of the profile with a higher gradient increased in depth, thus indicating the growth of the sea ice.

The sea-ice thickness was determined from the temperature profile and its corresponding freezing temperature (Fig. 5a). This model was able to give an estimate of the increase in sea-ice thickness. This preliminary evaluation of thickness assumed homogeneity throughout the growing sample and did not account for potential differences of thickness with the presence of equipment and the tank walls. The fastest growth rate happened early in the experiment, after which it slowed. The slowing rate was caused by the insulating effect of the thickening sea ice together with the salinity increase in the underlying saline solution during sea-ice growth from brine drainage (Weeks and Cox, 1974).

The bulk salinity profile of the sea ice at sampling can be seen in Figure 5b. This profile was constructed using the three samples from the tank, marked by  $I_{1,2,3}$  in Figure 4. The measured salinities were found to be similar to the laboratory-grown sea-ice bulk salinity measured by Wiese and others (2015) and the young, natural sea-ice bulk salinity measured by Eicken (1992). The profile shape is that of an S-shaped curve, typical of young sea ice (Eicken, 1992).

In the early set-up stages of the laboratory at MARiS, visualisation with cross-polarisation techniques were not available to use. Further improvement and development of equipment for visualisation is currently underway. However, preliminary  $\mu$ CT scans were available to assist in the visualisation of the sample structure to determine if the internal structure, namely the brine pore and channel arrangement, was like that of natural sea ice.

These scans were produced by a Phoenix v|tome|x micro-X-ray CT scanner at room temperature for a duration of 20 min at 35  $\mu$ m resolution. The temperature was not able to be controlled as the equipment was not in a cold room or laboratory, thus it was only possible to achieve viable images with 20 min of scanning time before the sample was compromised from melting. The samples were 3 cm<sup>3</sup> from the top and bottom sections of a laboratory-grown sea-ice specimen, which was 23 cm in length.  $\mu$ CT scans produce images in greyscale that allows one to differentiate features by their respective density. The resulting images,

shown in Figure 6, highlight the air pockets, brine channels and dendritic platelet growth within the laboratory sea ice. As air has a lower density compared to the solid ice, the air pockets are displayed as black spots marked by the red circles, while brine has a higher density, thus it is identified by the white inclusions marked by the yellow circles.

The images received from the top of the laboratory grown sea ice (Fig. 6a) showed rounded pore spaces with spotted brine inclusions. The brine inclusions were difficult to determine accurately. The distribution and general shape of the brine inclusions were rounded and sporadic, indicating a granular structure within the sea ice. Granular structures are typically found at the surface of natural sea ice whereby the growth conditions are erratic and more turbulent with fast-freezing conditions (Weeks and Ackley, 1986; Weeks, 2010).

The images taken from the bottom of the laboratory-grown sea-ice specimen (Fig. 6b) displayed the development of a columnar structure within the sea ice with elongated brine inclusions and air pockets. These elongated air pockets may be indicative of brine loss during sample extraction. Columnar structure is typical for sea ice formed under calm conditions whereby the crystals can align themselves perpendicular to their basal plane, to form long column-like crystals (Weeks, 2010). This texture was closely linked to the formation of brine channels throughout the sea ice (Fig. 6b).

#### 5.4 Evaluation of set-up

In summary, the laboratory sea ice grown within the small-scale system had many of the properties that classified it as sea ice. The sea ice had a vertical, linear temperature profile, with a square root function sea-ice thickness evolution. The preliminary  $\mu$ CT scan showed that the sea-ice crystal structure at the bottom of the sample consisted of vertically elongated crystals. The  $\mu$ CT scan also showed the location of brine inclusions as vertically orientated, contained within the intracrystalline planes. Lastly, the bulk salinity profile of the sea ice was observed to fit the S-shaped profile described within literature. The bulk salinity values were within range of that measured in young sea ice by

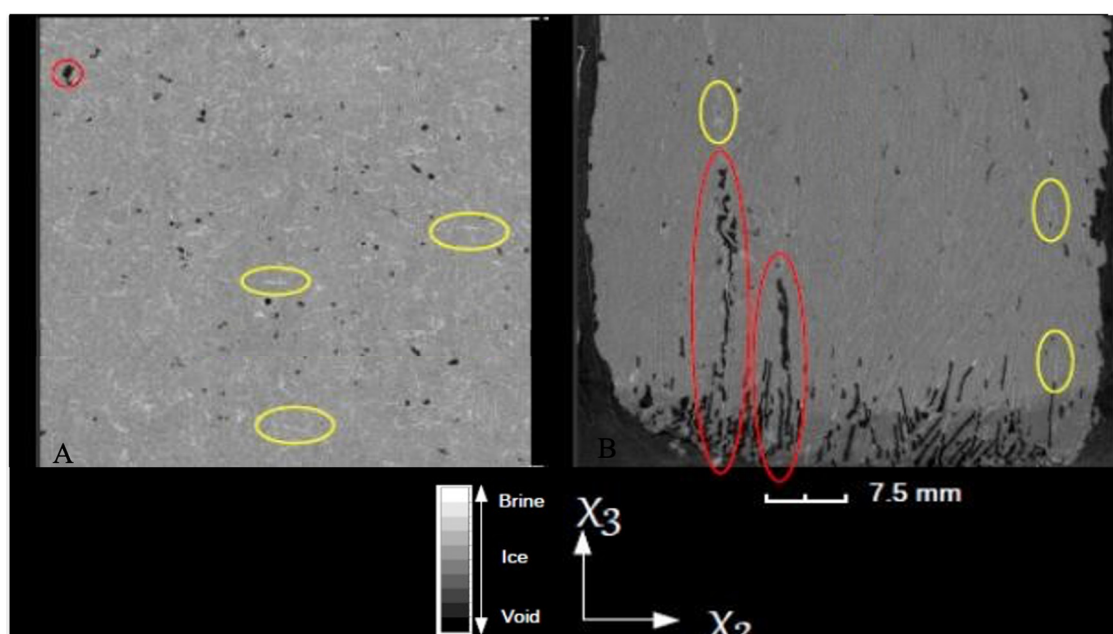


**Fig. 6.** Micro-X-ray CT scan images of 3 cm<sup>3</sup> sections of laboratory-grown sea ice in the X3–X2 plane, which views the sample from the side. Image A is from the top of the laboratory-grown specimen while image B is from the bottom of the specimen. The pore spaces are highlighted in red while the brine inclusions are highlighted in yellow.

Eicken (1992) and in laboratory studies by Wiese and others (2015). By fulfilling these key properties, the proof of design concept validated the tank system design with regards to its ability to usefully replicate the environmental conditions necessary to grow columnar sea ice in the laboratory. Therefore, the design objectives of the study have been met.

Further work is underway to improve this set-up and expand the scope of study on laboratory-grown sea ice. This includes the creation of a more permanent design with more temperature measurement equipment for higher horizontal and vertical spatial resolutions, external access to the data logger to reduce temperature fluctuations from entering and exiting the laboratory, and modification to the cooling fan and compressor unit to mitigate the need for defrost cycles.

## 6. Final remarks

This detailing of the major design considerations for laboratory sea-ice facilities aims at providing a starting point for the design of such a system. These design considerations were used when building the facility at the University of Cape Town and an experiment was performed to characterise the sea ice grown in this new facility. Salinity and temperature measurements as well as preliminary  $\mu$ CT scan images of the internal structure of the specimens are consistent with natural sea ice. The facilities discussed in this paper are by no means an exhaustive list and does not aim to provide a definitive methodology for creating laboratory sea ice. The exact requirements depend on the intended field of study, but it is recommended to properly determine the optimal selection for all the design considerations through an initial selection based on the desired sea-ice property of study, followed by careful iteration of each of the other design considerations.

**Acknowledgements.** This study was based on the research supported in part by the National Research Foundation of South Africa (NRF Grant No. 116801). We thank the research office at the University of Cape Town for their financial support. This publication is based on research that has been supported in part by the University of Cape Town's Research Committee (URC).

**Author contributions.** BH and TR wrote the original draft, SJ and BH edited the accepted first draft with reviews from TR and MT. BH performed the majority of the laboratory experiments with some assistance from SJ. BH and TR conducted the CT-scanning of the laboratory-grown samples. BH, MT and TR conceptualised this paper. TR provided supervision, funding and resources for the project.

## References

- Alberello A and 5 others (2019) An experimental model of wave attenuation in pancake ice. Proceedings of the 29th International Ocean and Polar Engineering Conference, ISOPE, 16 June–21 June 2019, Honolulu, Hawaii, 751–756.
- Backstrom LGE (2007) *Capacitance measurements of bulk salinity and brine movement in first-year sea ice* (MSc Thesis). University of Alaska, Fairbanks.
- Barrette PD and Jordaan IJ (2001) Compressive Behaviour of Confined Polycrystalline Ice. *Technical Report*, Ocean Engineering Research Centre, Memorial University of Newfoundland, St John's.
- Bogorodskiy PV and Marchenko AV (2014) Thermodynamic effects accompanying freezing of two water layers separated by a sea ice sheet. *Marine Physics* **54**, 170–177. doi: [10.1134/S0001437014020039](https://doi.org/10.1134/S0001437014020039)
- Buist I, Potter S, Nedwed T and Mullin J (2011) Herding surfactants to contract and thicken oil spills in pack ice for in situ burning. *Cold Regions Science and Technology* **67**(1–2), 3–23. doi: [10.1016/j.coldregions.2011.02.004](https://doi.org/10.1016/j.coldregions.2011.02.004)
- Bullock RJ, Aggarwal S, Perkins RA and Schnabel W (2017) Scale-up considerations for surface collecting agent assisted in-situ burn crude oil spill response experiments in the Arctic: laboratory to field-scale investigations. *Journal of Environmental Management* **190**, 266–273. doi: [10.1016/j.jenvman.2016.12.044](https://doi.org/10.1016/j.jenvman.2016.12.044)
- Cheng S, Tsarau A, Evers K-U and Shen H (2019) Floe size effect on gravity wave propagation through ice covers. *Journal of Geophysical Research: Oceans* **124**(1), 320–334. doi: [10.1029/2018JC014094](https://doi.org/10.1029/2018JC014094)
- Cottier F, Eicken H and Wadhams P (1999) Linkages between salinity and brine channel distribution. *Journal of Geophysical Research* **104**(C7), 15859–15871. doi: [10.1029/1999JC900128](https://doi.org/10.1029/1999JC900128)
- Cox GFN and Weeks WF (1975) Brine Drainage and Initial Salt Entrapment in Sodium Chloride Ice. *Technical Report*, Cold Regions Science and Technology Laboratory, Hanover, New Hampshire.
- Cox G and Weeks WF (1986) Changes in the salinity and porosity of sea ice samples during shipping and restorage. *Journal of Glaciology* **32**(112), 371–375. doi: [doi:10.3189/S0022143000012065](https://doi.org/10.3189/S0022143000012065)
- Crabeck O and 9 others (2016) Imaging air volume fraction in sea ice using non-destructive X-ray tomography. *The Cryosphere* **10**, 1125–1145. doi: [10.5194/tc-10-1125-2016](https://doi.org/10.5194/tc-10-1125-2016), 2016
- Dempsey JP, Wei Y, Defranco S, Ruben R and Frachetti R (1989). Fracture Toughness of S2 Columnar Freshwater Ice: Crack Length and Specimen Size Effects-Part 1. Proceedings of the 8th International Conference on Offshore Mechanics and Arctic Engineering. 19–23 March 1989. The Hague, The Netherlands. pp. 83–89.
- Dilliplaine K and 5 others (2021) Crude oil exposure reduces ice algal growth in a sea-ice mesocosm experiment. *Polar Biology* **44**, 525–537. doi: [10.1007/s00300-021-02818-3](https://doi.org/10.1007/s00300-021-02818-3)
- Dolatshah A and 6 others (2018) Hydroelastic interactions between water waves and floating freshwater ice. *Physics of Fluids* **30**(9), 091702. doi: [10.1063/1.5050262](https://doi.org/10.1063/1.5050262)
- Eicken H (1992) Salinity profiles of Antarctic sea ice: field data and model results. *Journal of Geophysical Research* **97**(C10), 15545–15557. doi: [10.1029/92JC01588](https://doi.org/10.1029/92JC01588)
- Eicken H, Bock C, Wittig R, Miller H and Poertner HO (2000) Magnetic resonance imaging of sea-ice pore fluids: methods and thermal evolution of pore microstructure. *Cold Regions Science and Technology* **31**(3), 207–255. doi: [10.1016/S0165-232X\(00\)00016-1](https://doi.org/10.1016/S0165-232X(00)00016-1)
- Eide LI and Martin S (1975) The formation of brine drainage features in young sea ice. *Journal of Glaciology* **14**(70), 137–154. doi: [10.3189/S0022143000013460](https://doi.org/10.3189/S0022143000013460)
- Feltham DL, Untersteiner N and Wettlaufer JS (2006) Sea ice is a mushy layer. *The Cryosphere* **33**(14), L14501. doi: [10.1029/2006GL026290](https://doi.org/10.1029/2006GL026290)
- Freitag J (1999) The hydraulic properties of Arctic sea ice: implications for the small-scale particle transport. *Berichte zur Polarforschung* **325**.
- Fuchs N (2017) *The impact of snow on sea-ice salinity* (MSc Thesis). University of Hamburg, Hamburg.
- Galley RJ and 6 others (2015) Imaged brine inclusions in young sea ice-shape, distribution and formation timing. *Cold Regions Science and Technology* **111**, 39–48. doi: [10.1016/j.coldregions.2014.12.011](https://doi.org/10.1016/j.coldregions.2014.12.011)
- Garnett J and 7 others (2019) Mechanistic insight into the uptake and fate of persistent organic pollutants in sea ice. *Environmental Science and Technology* **53**(2), 6757–6764. doi: [10.1021/acs.est.9b00967](https://doi.org/10.1021/acs.est.9b00967)
- Ghobrial TR, Loewen MR and Hicks F (2012) Laboratory calibration of upward looking sonars for measuring suspended frazil ice concentration. *Cold Regions Science and Technology* **70**, 19–31. doi: [10.1016/j.coldregions.2011.08.010](https://doi.org/10.1016/j.coldregions.2011.08.010)
- Golding N, Snyder SA, Schulson EM and Renshaw CE (2014) Plastic faulting in saltwater ice. *Journal of Glaciology* **60**(221), 447–452. doi: [10.3189/2014JG13J178](https://doi.org/10.3189/2014JG13J178)
- Griewank PJ and Notz D (2013) Insights into brine dynamics and sea ice desalination from a 1-D model study of gravity drainage. *Journal of Geophysical Research: Oceans* **118**(7), 3370–3386. doi: [10.1002/jgrc.20247](https://doi.org/10.1002/jgrc.20247)
- Gully A, Backstrom LGE, Eicken H and Golden KM (2007) Complex bounds and microstructural inversion for measurements of sea ice permittivity. *Physica B: Condensed Matter* **394**(2), 357–362. doi: [10.1016/j.physb.2006.12.067](https://doi.org/10.1016/j.physb.2006.12.067)
- Haas C (1999) Ice tank investigations of the microstructure of artificial sea ice grown under different boundary conditions during INTERICE II. Proceedings of HYDRALAB workshop, 19th February 1999, Germany.
- Hare AA and 5 others (2013) pH evolution in sea ice grown at an outdoor experimental facility. *Marine Chemistry* **154**, 46–54. doi: [10.1016/j.marchem.2013.04.007](https://doi.org/10.1016/j.marchem.2013.04.007)
- Hill JR and Lasca NP (1971) An improved method for determining ice fabrics. *Journal of Glaciology* **10**(38), 133–138. doi: [10.3189/S0022143000013071](https://doi.org/10.3189/S0022143000013071)
- Hirayama, K (1983) Properties of urea-doped ice in the CRREL test basin. *Technical Report*, Cold Regions Research and Engineering Laboratory, Hanover, New Hampshire.

- Hunke EC, Notz D, Turner AK and Vancoppenolle M (2011) The multi-phase physics of sea ice: a review for model developers. *The Cryosphere* 5(4), 989–1009. doi: [10.5194/tc-5-989-2011](https://doi.org/10.5194/tc-5-989-2011)
- Intergovernmental Panel on Climate Change (IPCC) (2007) Climate change 2007: The Physical Science Basis. Contributions of Working Group I to the Fourth Assessment Report of the Intergovernmental Panel on the Climate Change. Cambridge, Cambridge University Press.
- Kawamura T, Ishikawa M, Kojima S and Shirasawa K (2006) Measurements of Permeability of Sea Ice. Proceedings of the 18th IAHR International Symposium on Ice.
- Kim JH, Choi KS and Seo YK (2006) Standardization of laboratory experimental techniques with a cold room in Korea. *Journal of Ocean Engineering and Technology* 21(2), 60–66 (in Korean).
- Kuehn GA, Lee RW, Nixon WA and Schulson EM (1990) The structure and tensile behavior of first-year sea ice and laboratory-grown saline ice. *Journal of Offshore Mechanics and Arctic Engineering* 112(4), 357–363. doi: [10.1115/1.2919878](https://doi.org/10.1115/1.2919878)
- Kuehn GA and Schulson EM (1994) The mechanical properties of saline ice under uniaxial compression. *Annals of Glaciology* 19, 39–48. doi: [10.3189/1994AoG19-1-39-48](https://doi.org/10.3189/1994AoG19-1-39-48)
- Lake RA and Lewis EL (1970) Salt rejection by sea ice during growth. *Journal of Geophysical Research* 75(3), 583–597. doi: [10.1029/JC075i003p00583](https://doi.org/10.1029/JC075i003p00583)
- Lange MA, Ackley SF, Wadhams P, Dieckmann G and Eicken H (1989) Development of sea ice in the Weddell Sea. *Annals of Glaciology* 12, 92–96. doi: [10.3189/S0260305500007023](https://doi.org/10.3189/S0260305500007023)
- Langhorne PJ and Robinson W (1986) Alignment of crystals in sea ice due to fluid motion. *Cold Regions Science and Technology* 12(2), 197–214. doi: [10.1016/0165-232X\(86\)90033-9](https://doi.org/10.1016/0165-232X(86)90033-9)
- Langway Jr CC (1958) Ice Fabrics and the Universal Stage. *Technical Report* 62, U.S. Army Snow Ice and Permafrost Research Establishment, Corps of Engineers, Wilmette, Illinois.
- Lekang OI (2013) *Aquaculture Engineering*. Oxford: John Wiley and Sons.
- Li H, Gedikli ED and Lubbad R (2021) Laboratory study of wave-induced flexural motion of ice floes. *Cold Regions Science and Technology* 182, 103208. doi: [10.1016/j.coldregions.2020.103208](https://doi.org/10.1016/j.coldregions.2020.103208)
- Li H and Lubbad R (2018) Laboratory Study of Ice Floes Collisions under Wave Action. Proceedings of the Twenty-eighth (2018) International Ocean and Polar Engineering Conference, 10th June 2018, Sapporo, Japan.
- Liang K and 5 others (2004) Examination of the process scale dependence of L-glutamic acid batch crystallized from supersaturated aqueous solutions in relation to reactor hydrodynamics. *Industrial and Engineering Chemistry Research* 43(5), 1227–1234. doi: [10.1021/ie0305014](https://doi.org/10.1021/ie0305014)
- Light B, Carns RC and Warren SG (2015) ‘Albedo dome’: a method for measuring spectral flux-reflectance in a laboratory for media with long optical paths. *Applied Optics* 54(17), 5260–5269. doi: [10.1364/ao.54.005260](https://doi.org/10.1364/ao.54.005260)
- Loose B, McGillis WR, Schlosser P, Perovich D and Takahashi T (2009) Effects of freezing, growth, and ice cover on gas transport processes in laboratory seawater experiments. *Geophysical Research Letters* 36(5), 1–5. doi: [10.1029/2008GL036318](https://doi.org/10.1029/2008GL036318)
- Loose B, Miller LA, Elliott S and Papakyriakou T (2011) Sea ice biogeochemistry and material transport across the frozen interface. *Oceanography* 24(3), 202–218. doi: [10.5670/oceanog.2011.72](https://doi.org/10.5670/oceanog.2011.72)
- Marchenko A and 7 others (2021) Laboratory investigations of the bending rheology of floating saline ice and physical mechanisms of wave damping in the HVA Hamburg ship model basin ice tank. *Water* 13(8), 1080. doi: [10.3390/w13081080](https://doi.org/10.3390/w13081080)
- Marchenko A, Lishman B, Wrangborg D and Thiel T (2016) Thermal expansion measurements in fresh and saline ice using fiber optic strain gauges and multipoint temperature sensors based on Bragg gratings. *Journal of Sensors* 2016(103), 1–13. doi: [10.1155/2016/5678193](https://doi.org/10.1155/2016/5678193)
- Marchenko A, Shestov S, Sigitov A and Løset S (2011) Water-Ice Actions on the Coal Quay at Kapp Amsterdam in Svalbard. Proceedings of the 21st International Conference on Port and Ocean Engineering under Arctic Conditions, 10–14th July 2011, Montreal, Canada.
- Marks AA, Lamare ML and King MD (2017) Optical properties of laboratory grown sea ice doped with light absorbing impurities (black carbon). *The Cryosphere* 11, 2867–2881. doi: [10.5194/tc-2017-76](https://doi.org/10.5194/tc-2017-76)
- Maykut GA and Untersteiner N (1971) Some results from a time-dependent thermodynamic model of sea ice. *Journal of Geophysical Research* 76(6), 1550–1575. doi: [10.1029/JC076i006p01550](https://doi.org/10.1029/JC076i006p01550)
- McFarlane V, Loewen M and Hicks F (2015) Measurements of the evolution of frazil ice particle size distributions. *Cold Regions Science and Technology* 120, 45–55. doi: [10.1016/j.coldregions.2015.09.001](https://doi.org/10.1016/j.coldregions.2015.09.001)
- Middleton CA, Thomas C, De Wit A and Tison J-L (2016) Visualizing brine channel development and convective processes during artificial sea-ice growth using Schlieren optical methods. *Journal of Glaciology* 62(231), 1–17. doi: [10.1017/jog.2015.1](https://doi.org/10.1017/jog.2015.1)
- Murda A, Schulson EM and Renshaw CE (2021) Behavior of saline ice under cyclic flexural loading. *The Cryosphere* 15(5), 2415–2428. doi: [10.5194/tc-15-2415-2021](https://doi.org/10.5194/tc-15-2415-2021)
- Naumann AK, Notz D, Havik L and Sirevaag A (2012) Laboratory study of initial sea-ice growth: properties of grease ice and nilas. *The Cryosphere* 6(4), 729–741. doi: [10.5194/tc-6-729-2012](https://doi.org/10.5194/tc-6-729-2012)
- Nelli F and 6 others (2017) Reflection and transmission of regular water waves by a thin floating plate. *Wave Motion* 70, 209–221. doi: [10.1016/j.wavemoti.2016.09.003](https://doi.org/10.1016/j.wavemoti.2016.09.003)
- Nomura D, Yoshikawa-Inoue H and Toyota T (2006) The effect of sea-ice growth on air–sea CO<sub>2</sub> flux in a tank experiment. *Tellus B: Chemical and Physical Meteorology* 58(5), 418–426. doi: [10.1111/j.1600-0889.2006.00204.x](https://doi.org/10.1111/j.1600-0889.2006.00204.x)
- Notz D, Wettlaufer JS and Worster M (2005) A non-destructive method for measuring the salinity and solid fraction of growing sea ice in situ. *Journal of Glaciology* 51, 159–166.
- Notz D and Worster MG (2006) A one-dimensional enthalpy model of sea ice. *Annals of Glaciology* 44, 123–128. doi: [10.3189/172756406781811196](https://doi.org/10.3189/172756406781811196)
- Notz D and Worster MG (2008) In situ measurements of the evolution of young sea ice. *Journal of Geophysical Research: Oceans* 113(3), C03001. doi: [10.1029/2007JC004333](https://doi.org/10.1029/2007JC004333)
- Oggier M, Eicken H, Wilkinson J, Petrich C and O’Sadnick M (2019) Crude oil migration in sea-ice: laboratory studies of constraints on oil mobilization and seasonal evolution. *Cold Regions Science and Technology* 174, 102924. doi: [10.1016/j.coldregions.2019.102924](https://doi.org/10.1016/j.coldregions.2019.102924)
- Omega (2019) Thermocouple types. Available at <https://www.omega.com/en-us/resources/thermocouple-types>.
- Papadimitriou S, Kennedy H, Kattner G, Dieckmann GS and Thomas DN (2004) Experimental evidence for carbonate precipitation and CO<sub>2</sub> degassing during sea ice formation. *Geochimica et Cosmochimica Acta* 68(8), 1749–1761. doi: [10.1016/j.gca.2003.07.004](https://doi.org/10.1016/j.gca.2003.07.004)
- Passerotti G and 9 others (2020) Wave Propagation in Continuous Sea Ice: An Experimental Perspective. Proceedings of the 39th International Conference on Ocean, Offshore and Arctic Engineering (OMAE), 3–7 August 2020, Virtual, Online. doi: [10.1115/OMAE2020-18181](https://doi.org/10.1115/OMAE2020-18181)
- Passerotti G and 7 others (2022) Interactions between irregular wave fields and sea ice: a physical model for wave attenuation and ice break up in an ice tank. *Journal of Physical Oceanography* 52(7), 1431–1446. doi: [10.1175/JPO-D-21-0238.1](https://doi.org/10.1175/JPO-D-21-0238.1)
- Perovich DK and Grenfell TC (1981) Laboratory studies of the optical properties of young sea ice. *Journal of Glaciology* 27(96), 329–344. doi: [10.3189/S0022143000015410](https://doi.org/10.3189/S0022143000015410)
- Petrich C and Eicken H (2010) Growth, structure and properties of sea ice. In Thomas DN and Dieckmann G eds. *Sea Ice*. West Sussex, United Kingdom: Wiley-Blackwell, pp. 23–77.
- Rabault J, Sutherland G, Jensen A, Christensen KH and Marchenko A (2019) Experiments on wave propagation in grease ice: combined wave gauges and particle image velocimetry measurements. *Journal of Fluid Mechanics* 864, 876–898. doi: [10.1017/jfm.2019.16](https://doi.org/10.1017/jfm.2019.16)
- Randall D, Nathoo J and Lewis A (2009) Seeding for selective salt recovery during eutectic freeze crystallization. Proceedings of International Mine Water Conference, 19–23 October 2009, Pretoria, South Africa, pp. 639–646.
- Rees Jones DW and Worster MG (2014) A physically based parameterization of gravity drainage for sea-ice modeling. *Journal of Geophysical Research: Oceans* 119(9), 5599–5621. doi: [10.1002/2013JC009296](https://doi.org/10.1002/2013JC009296)
- Roscoe HK and 6 others (2011) Frost flowers in the laboratory: growth, characteristics, aerosol, and the underlying sea ice. *Journal of Geophysical Research Atmospheres* 116(12), 1–12. doi: [10.1029/2010JD015144](https://doi.org/10.1029/2010JD015144)
- Rysgaard S and 14 others (2014) Temporal dynamics of ikaite in experimental sea ice. *The Cryosphere* 8(4), 1469–1478. doi: [10.5194/tc-8-1469-2014](https://doi.org/10.5194/tc-8-1469-2014)
- Sammonds P, Hatton D and Feltham D (2017) Micromechanics of sea ice frictional slip from test basin scale experiments. *Philosophical Transactions of the Royal Society A: Mathematical, Physical and Engineering Sciences* 375(2086), 20150354. doi: [10.1098/rsta.2015.0354](https://doi.org/10.1098/rsta.2015.0354)
- Schneck CC, Ghobrial TR and Loewen MR (2019) Laboratory study of the properties of frazil ice particles and flocs in water of different salinities. *The Cryosphere* 13, 2751–2769. doi: [10.5194/tc-2019-99](https://doi.org/10.5194/tc-2019-99)

- Schulson EM, Renshaw CE and Synder SA** (2015) Effect of Deformation Damage on the Mechanical Behavior of Sea Ice: Ductile–Brittle Transition, Elastic Modulus and Brittle Compressive Strength. *Final Report*, Ice Research Laboratory, Dartmouth College, Hanover, New Hampshire.
- Schwarz J** and 7 others (1981) Standardized testing methods for measuring mechanical properties of ice. *Cold Regions Science and Technology* **4**(3), 245–253. doi: [10.1016/0165-232X\(81\)90007-0](https://doi.org/10.1016/0165-232X(81)90007-0)
- Shaw MD, Carpenter LJ, Baeza-Romero MT and Jackson AV** (2011) Thermal evolution of diffusive transport of atmospheric halocarbons through artificial sea-ice. *Atmospheric Environment* **45**(35), 6393–6402. doi: [10.1016/j.atmosenv.2011.08.023](https://doi.org/10.1016/j.atmosenv.2011.08.023)
- Shen H, Evers K-U, Ackley SF, Dai M and Wilkinson J** (2003) Salinity and Porosity of Laboratory Grown Young Pancakes. Proceedings of the 17th International Conference on Port and Ocean Engineering Under Arctic Conditions, 16–19 June 2003, Trondheim, Norway.
- Shirtcliffe TGL, Huppert HE and Worster MG** (1991) Measurement of the solid fraction in the crystallization of a binary melt. *Journal of Crystal Growth* **113**(3–4), 566–574. doi: [10.1016/0022-0248\(91\)90092-J](https://doi.org/10.1016/0022-0248(91)90092-J)
- Shokr M, Asmus K and Agnew T** (2009) Microwave emission observations from artificial thin sea ice: the ice-tank experiment. *IEEE Transactions on Geoscience and Remote Sensing* **47**(1), 325–338. doi: [10.1109/TGRS.2008.2005585](https://doi.org/10.1109/TGRS.2008.2005585)
- Stander E and Michael B** (1989) The effect of fluid flow on the development of preferred orientations in sea ice: laboratory experiments. *Cold Regions Science and Technology* **17**(2), 153–161. [https://doi.org/10.1016/S0165-232X\(89\)80005-9](https://doi.org/10.1016/S0165-232X(89)80005-9).
- Style RW and Worster MG** (2009) Frost flower formation on sea ice and lake ice. *Geophysical Research Letters* **36**(11), 20–23. doi: [10.1029/2009GL037304](https://doi.org/10.1029/2009GL037304)
- Sutherland G, Rabault J, Christensen KH and Jensen A** (2019) A two-layer model for wave dissipation in sea ice. *Applied Ocean Research* **88**, 111–118. doi: [10.1016/j.apor.2019.03.023](https://doi.org/10.1016/j.apor.2019.03.023)
- Thomas M** and 6 others (2020) Tracer measurements in growing sea ice support convective gravity drainage parameterizations. *Journal of Geophysical Research* **125**(2), e2019JC01579. doi: [10.1029/2019JC015791](https://doi.org/10.1029/2019JC015791).
- Thomas M** and 10 others (2021) The Roland von Glasow Air-Sea-Ice Chamber (RvG-ASIC): an experimental facility for studying ocean/sea-ice/atmosphere interactions. *Atmospheric Measurement Techniques Discussions* **14**(3), 1833–1849. doi: [10.5194/amt-14-1833-2021](https://doi.org/10.5194/amt-14-1833-2021)
- Timco G and Weeks WF** (2010) A review of the engineering properties of sea ice. *Cold Regions Science and Technology* **60**(2), 107–129. doi: [10.1016/j.coldregions.2009.10.003](https://doi.org/10.1016/j.coldregions.2009.10.003)
- Timmons MB, Summerfelt ST and Vinci BJ** (1998) Review of circular tank technology and management. *Aquacultural Engineering* **18**(1), 51–69. doi: [10.1016/S0144-8609\(98\)00023-5](https://doi.org/10.1016/S0144-8609(98)00023-5)
- Tucker III W, Gow A and Weeks WF** (1987) Physical properties of summer sea ice in the Fram Strait. *Journal of Geophysical Research* **92**(C7), 6787–6803 (doi: [10.1029/JC092iC07p06787](https://doi.org/10.1029/JC092iC07p06787))
- Turner AK, Hunke EC and Bitz CM** (2013) Two modes of sea-ice gravity drainage: a parameterization for large-scale modeling. *Journal of Geophysical Research: Oceans* **118**(5), 2279–2294. doi: [10.1002/jgrc.20171](https://doi.org/10.1002/jgrc.20171)
- van der Elsken J, Dings J and Michielsen JCF** (1991) The freezing of super-cooled water. *Journal of Molecular Structure* **250**(2–4), 245–251. doi: [10.1016/0022-2860\(91\)85031-W](https://doi.org/10.1016/0022-2860(91)85031-W)
- Weeks WF** (1962) Tensile strength of NaCl ice. *Journal of Glaciology* **4**(31), 25–52. doi: [10.3189/S0022143000018190](https://doi.org/10.3189/S0022143000018190)
- Weeks WF** (2010) *On Sea Ice*. Fairbanks: University of Alaska Press.
- Weeks WF and Ackley SF** (1986) The growth, structure and properties of sea ice. In Untersteiner N ed. *The Geophysics of Sea Ice*. Boston: Springer, pp. 9–164.
- Weeks WF and Assur A** (1967) *The Mechanical Properties of Sea Ice*. Report, Cold Regions Research and Engineering Laboratory, Hanover, New Hampshire.
- Weeks WF and Cox G** (1974) Laboratory Preparation of Artificial Sea and Salt Ice. Report, Cold Regions Research and Engineering Laboratory, Hanover, New Hampshire.
- Weissenberger J, Dieckmann D, Gradinger R and Spindler M** (1992) Sea ice: a cast technique to examine and analyze brine pockets and channel structure. *Limnology and Oceanography* **37**(1), 179–183. doi: [10.4319/lo.1992.37.1.0179](https://doi.org/10.4319/lo.1992.37.1.0179)
- Wiese M** (2012) *Laboratory experiments on the thermodynamics of melting sea ice* (MSc Thesis). University of Hamburg, Hamburg.
- Wiese M, Griewank P and Notz D** (2015) On the thermodynamics of melting sea ice versus melting freshwater ice. *Annals of Glaciology* **56**(69), 191–199. doi: [10.3189/2015AoG69A874](https://doi.org/10.3189/2015AoG69A874)
- Wilkinson JP** and 14 others (2009) *Eos* **90**(10), 81–82. doi: [10.1029/2009EO100002](https://doi.org/10.1029/2009EO100002)
- Ye SQ and Doering J** (2004) Simulation of the supercooling process and frazil evolution in turbulent flows. *Canadian Journal of Civil Engineering* **31**(6), 915–926. doi: [10.1139/l04-055](https://doi.org/10.1139/l04-055)
- Zeigermann LM** (2018) *Desalination Processes of Thin Sea Ice During Freezing and Melting* (MSc Thesis). University of Hamburg, Hamburg.